*REPRINTED FROM 'THE PHYSICS AND CHEMISTRY OF HIGH PRESSURES'*

# THE PRESSURE VARIATION OF THE ELASTIC CONSTANTS OF CRYSTALS

By W. B. DANIELS

(*Princeton University, Princeton, New Jersey, U.S.A.*)

and

CHARLES S. SMITH

(*Case Institute of Technology, Cleveland, Ohio, U.S.A.*)

Measurement of the pressure-dependence of elastic constants of crystals yields information pertinent to the experimental equation of state of solids, to theories of cohesion of solids, and to certain aspects of anharmonicity of lattice vibrations in solids. This paper discusses some of the information which has been provided by such measurements carried out on copper, silver, gold, aluminium, sodium, lithium, germanium, silicon and rubidium iodide. Experimental aspects are presented, and a few suggestions are made for extending the direct measurements of anharmonicity of lattice vibrations.

## Introduction

The compressibility and variation of compressibility of crystals with pressure has long been the subject of quantitative experimental investigation by Bridgman whose results have provided the basis of many theoretical investigations of cohesion, notable among these are the works of Wigner & Seitz,[1] Frohlich,[2] and Bardeen[3,4] on compression of the alkali metals. Implications about the thermal properties of solids have been based on Bridgman's dilatational data, especially by Slater[5] whose establishment of the relation between Grüneisen's gamma and the pressure-dependence of the compressibility is familiar. Swenson is making very careful and elegant measurements of the compression of solids over a wide range of temperatures down to almost liquid helium temperature to obtain experimentally, temperature-dependent equations of state.[6] One may reasonably ask then whether it is worth while investigating the pressure-dependence of the shear elastic constants of crystals as well as that of the bulk modulus. It is hoped that the following discussion will serve to introduce the experimental aspects of the subject and to justify its pursuit by a brief indication of the sort of information about crystal binding forces and about anharmonic thermal properties of solids which reveals itself in interpretation of the data.

At the present time, few measurements have been made in this field. The pressure-dependence of the shear stiffnesses of a few polycrystalline solids has been studied by Birch,[7] and by Hughes.[8,9] Lazarus[10] in a pioneering paper reports on studies on single crystals of potassium and sodium chloride, copper–zinc, copper and aluminium with the ultrasonic pulse echo method. Very careful measurements on pressure- and temperature-dependence of elastic constants of germanium have been made by McSkimmin,[11] and mention must be made of the interesting work done by Anderson[12] seeking values of thermodynamic functions by measurements of the pressure- and temperature-dependence of the elastic constants of fused silica. Some interesting Russian work has appeared on the pressure-dependence of the elastic constants of cerium through the phase transition pressure at about 7·6 kb.[13] The remainder of the investigations, including those of copper, silver, gold,[14] aluminium, magnesium,[15] silicon,[16] sodium[17] and lithium[18] have been done at Case Institute of Technology, and our group at Princeton is engaged at the moment in the study of rubidium iodide.[19]

This paper is divided into three parts; (1) a discussion of techniques of measurement; (2) the interpretation of the results in terms of the various contributions to the cohesive energy of crystals; and (3) the implications of the results regarding the anharmonic thermal properties of solids. Some limitations and extensions of the methods will be considered briefly.

## (1) Experimental methods

Most of the results to be discussed in this paper were obtained by the ultrasonic pulse echo method of measuring elastic constants.[20,21] This non-resonant method is well suited to the problems associated with an ambient consisting of a fluid at high pressure, but is probably less accurate than the phase comparison method used by McSkimmin[22] and Anderson.[12] Only the ultrasonic pulse echo method is considered here: for a discussion of other methods of measuring elastic constants reference should be made to Huntington's review article.[23]

The apparatus required for these experiments consists of a pressure-generating and measuring system, and a thick-walled steel vessel of sufficient size to contain the sample crystal, with one

electric lead in for the pulsed radio-frequency (r.f.). The pressure-generating system used for most of the measurements has been a fairly conventional pump with intensifier,[24] but a new system incorporating only a direct pump has been used to 5kb with complete reliability, with occasional runs to 10kb. It uses a re-entrant seal[25] on the critical high-pressure piston closure. Seals at other closures have been effected using armoured O-rings.[25] A manganin wire coil with nominal resistance 300 ohms has been used as the pressure sensor,[26] a conventional Wheatstone bridge being used to measure the changes of its resistance. The freezing pressure of mercury at 0°, 7640 kg/cm.$^2$ after Bridgman,[26] has been taken as the high-pressure fixed point. Electrical leads have been made with the conventional Bridgman pipestone cones[27] and with careful fitting have proven completely reliable. Di-2-ethylhexyl sebacate (Octoil-S* or Plexol 201†) has been used as pressure fluid except for work with the alkali metals, where the high chemical reactivity demanded use of an isobutane–mineral oil mixture. The sebacate has the advantages of excellent lubricity and a low pressure coefficient of viscosity (silicone fluids are poor on both these points). All the above equipment has functioned for long periods of time with a minimum of maintenance.

Fig. 1 is a block diagram of the electronic components of a typical (and commercially available) ultrasonic pulse echo setup for measuring elastic constants of single crystals. The measurement to be made is basically one of time of travel of a pulse of 10 mc acoustic waves down the sample and back. The time mark generator is the heart of the apparatus, producing a set of markers to which the time measurements are referred. Stable markers are controlled by an oscillating quartz crystal maintained at constant temperature by an oven to assure its frequency stability. In operation, the time mark generator triggers simultaneously the pulse generator which emits about a 1 $\mu$sec. burst of 10 mc oscillations, and the sweep of high speed oscilloscope. The pulse of r.f. excites a 10 mc resonant X- or Y-cut quartz transducer cemented to the specimen crystal, generating an acoustic pulse of appropriate polarisation which echoes back and forth in the crystal. A variable sweep delay network on the oscilloscope calibrated against the time mark generator, enables precise measurements of the pulse transit time and especially of the *change* of transit time with pressure or any other independent variable. An invaluable improvement in technique for measuring changes of transit time was introduced by Eros & Reitz[28] who altered the electronics to permit display of the unrectified pulse whereas previously only the pulse envelope could be displayed. This removed the problem caused by changes of pulse shape with pressure.

The equation of motion describing the passage of an elastic wave through the crystal yields equations of the form $C = \rho v^2$, where $\rho$ is the density of the crystal, $v$ the velocity of the wave under consideration and $C$ is the stress–strain ratio for the specific distortion caused by passage of that wave.[29] (The derivation, made treating the crystal as an elastic continuum is of course valid only if the wavelength is very much larger than the inter-ionic spacing, a condition rigorously met by the 10-mc disturbances applied in the measurements.) For a cubic crystal cut with [110]

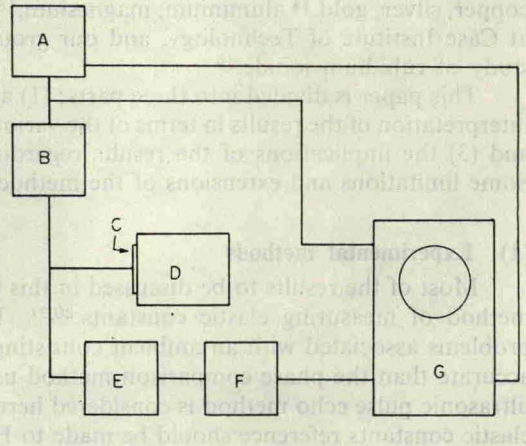


Fig. 1. *Block diagram of ultrasonic pulse echo components*

A Time mark generator (Tektronix TM 181 with crystal oven) B Pulse generator (Arenberg PG–650C) C quartz crystal transducer D single crystal sample E pre-amplifier (Arenberg PA–620–SN) F wide band amplifier (Arenberg WA–600–B) G oscilloscope (Tektronix Model 585 with Type CA dual traced plug-in unit. The Oscilloscope sweep delay helipot has been replaced by a more sensitive voltage divider)

* Octoil–S is a vacuum diffusion pump fluid sold by Consolidated Electrodynamics Corp., Rochester, New York.
† Plexol 201 is available from Rohm & Haas Chemical Co., Resinous Products Division, Philadelphia 5, Pa, U.S.A.

acoustic faces (see Fig. 2), the complete set of three independent elastic constants $C \equiv C_{44}$, $C' \equiv 1/2\,(C_{11} - C_{12})$ and $C_{11}' \equiv C_{11} - C' + C$, are given directly by $\rho v_i^2$ where the $v_i$ for the three constants $C$, $C'$ and $C_{11}'$ are the values for (i) a transverse wave with particle motion along the [001] direction (C), (ii) a transverse wave with particle motion along [110]($C'$) and (iii) a longitudinally polarised wave ($C_{11}'$). Then the adiabatic bulk modulus $B_s = C_{11}' - C_{44} - 1/3C'$. For the usual metallic anisotropies, $C > C'$, somewhat greater precision of the measurement of $B_s$ may be obtained by use of a second crystal with [100] orientation. Then $C_{11} = \rho v^2$ for the longitudinal wave, and $B_s = C_{11} - 4/3\ C'$, usually a relatively small correction from the direct measurement, e.g. about 20% in the case of silver, 12% in sodium, is necessary. The acoustic wave velocities are of course the quotients of twice the length of the sample between acoustic faces ($L$), and the transit time $t$ of a pulse, measured with the calibrated sweep delay, i.e. $C = \rho 4L^2/t^2$. If the pressure is changed, $\rho$, $L$ and $t$ change, yielding $\dfrac{\mathrm{d}\ln C}{\mathrm{d}P} = + \dfrac{1}{3B_T} - \dfrac{2}{t} \cdot \dfrac{\mathrm{d}t}{\mathrm{d}P}$ for small changes. The first term arises from changes of $L$ and $\rho$ with pressure. The isothermal bulk modulus must be computed from the measured adiabatic bulk modulus from the thermodynamic relation

$$B_s = B_T \left(1 + \frac{TV\beta^2 B_T}{Cv}\right)$$

where $\beta$ is the volume coefficient of thermal expansion, $T$ the absolute temperature, $Cv$ and $V$ the heat capacity and volume per mole. The second term is given by the data taken, i.e. *change* of transit time with pressure. In our technique the change is always measured with respect to a nearby time marker to reduce any effects due to time zero drift. Figs. 3 and 4 show typical curves of change of time of echo arrival relative to a nearby time marker *versus* change of the coil resistance of the pressure gauge, the latter being proportional to pressure change. [Note the complete absence of hysteresis between points taken with increasing pressure and those taken with decreasing pressure. This is important because it is contrary to the assumption that length hysteresis is a natural phenomenon in most samples, even if the pressure is truly hydrostatic.[6] The assumption is based on observation of apparent hysteresis of length in compression determinations made with lever piezometers, and seems to indicate the presence of friction somewhere in the length-measuring apparatus.] From these data and values of the constants at zero pressure, we calculate the quantities $\mathrm{d}C/\mathrm{d}P$ or the more characteristic quantity $\mathrm{d}\ln C/\mathrm{d}\ln r = -\dfrac{3B_T}{C} \cdot \dfrac{\mathrm{d}C}{\mathrm{d}P}$ which is given the title the ' logarithmic hydrostatic strain derivative ' or just ' strain derivative '. The precision of such measurements has recently been investigated extensively by Corll and Smith at Case Institute on single crystals of silver, with orientations [100], [110] and [111], confirming earlier estimates of about 0·3% in the $C$, 3% in the derivatives.[30] The precision will of course be higher in the more compressible materials for which the change in the stiffness is large over the pressure range used; and lower for materials less compressible than silver. This precision is we think remarkable and implies that the use of ultrasonic methods to obtain equations of state of solids deserves serious consideration, yet the only serious work in such a direction is that of Anderson[12] on fused silica. Our own measurements have been completely aimed at finding derivatives, and attempting to evaluate them at zero pressure. Thus, in the case of sodium, the data taken were arbitrarily confined to a pressure range less than 2kb and no special attempt was made

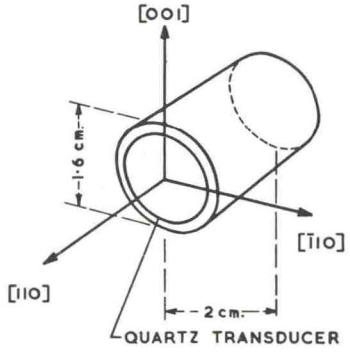


Fig. 2. *Typical specimen size and shape* X- or Y-cut quartz crystal transducers generate longitudinal or transverse waves respectively

to interpret the data in terms of $\triangle V/V$ over a wide range of pressures. Measurements taken over the more extended range to 7·8 kb revealed no difficulty (see Fig. 4), and indeed no real problem should appear in extending such measurements to a much higher pressure or to higher or lower temperatures. The employment of a larger model of the Swenson modification[31] of the high-pressure apparatus of Dugdale & Hulbert[32] for use at temperatures near 4·2°K should even permit very accurate $PV$ measurements to be made acoustically (in materials which do not have structure transformations) in this temperature range. As will be seen in the third section of this paper, the breakdown of the assumption that Poisson's ratio is independent of pressure is very serious in discussions of the lattice contribution to the thermal expansion. Yet, if one uses $P$–$V$ data alone as Slater was forced to do (for lack of shear data), no knowledge of pressure dependence of the Poisson ratios is obtained. Further, regarding accuracy of measurements $\triangle V$ vs $P$ reference is made to pp. 83—85 of Swenson's recent review article.[6] We agree completely that the best $\triangle V$ vs $P$ data can be provided by careful acoustic measurements. A discussion of the use of the acoustic method for determining parameters of the equation of state and values of thermodynamic functions, is given by Anderson.[12] It is suggested that those who contemplate highly refined $P$–$V$–$T$ measurements on solids, at least for those cases where single crystals may be obtained, should consider whether extension of this method to low temperatures using techniques perfected by Swenson[6] or to high temperatures using a stepped crystal as has been done by Bernstein,[33] would not produce results sufficiently more reliable than those obtained by direct compression of polycrystalline materials to warrant the additional effort required.

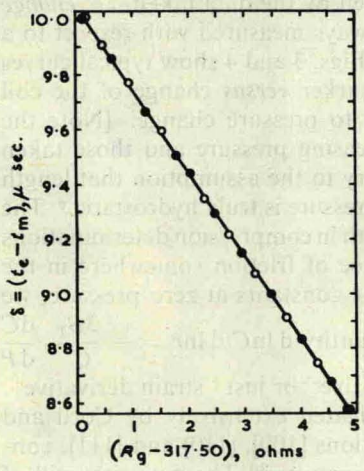


Fig. 3. *Typical data plot showing difference between the time,* $t_e$, *of arrival of one of the maxima of echo No. 7 of the longitudinal wave in a* 3·164 cm. *long aluminium crystal and a fixed time-marker,* $t_m$, *as a function of pressure-gauge coil resistance,* $R_g$

● increasing pressure ○ decreasing pressure

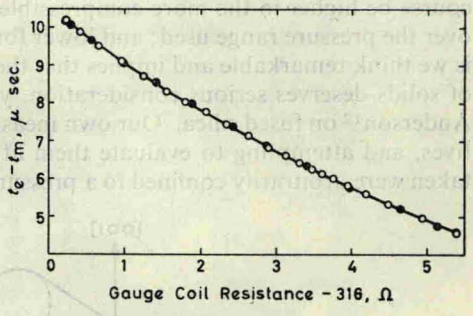


Fig. 4. *Change with pressure of the time of arrival of an echo for the* $C_{44}$ *wave in sodium*

The pressure range indicated is about 7800 bars

**(2) Interpretation of data**

To introduce the subject of interpretation of the data obtained in terms of lattice interactions, consider Table I which gives values of the elastic constants and their strain derivatives for a variety of materials.

The measurements have all been made at room temperature. Values for germanium were measured by McSkimmin at the Bell Laboratories and for rubidium iodide at the Princeton University and the remainder at the Case Institute of Technology. Note that dimensionally elastic constants have the form $e^2/r^4$ where $e$ is the electron charge and $r$ a linear dimension.

The coulomb contribution to the elastic constants arises from the change of the classical electrostatic energy of a structure by strain, assuming that no re-distribution of charge is brought about by the strain. *Analytically*, the coulomb contribution to the elastic constants has the form $e^2/r^4$. For example, in the case of the sodium chloride structure, the coulomb contributions to $C$ and $C'$ are $C_{\text{coul}} = \frac{1{\cdot}28}{2} \cdot \frac{e^2}{R^4}$ and $C'_{\text{coul}} = -\frac{1{\cdot}33}{2} \cdot \frac{e^2}{R^4}$ where $R$ is the cation–anion separation in the crystal. For this important contribution to the elastic constants, $\frac{\mathrm{d} \ln C}{\mathrm{d} \ln r} = -4$. Experimentally, it is observed that the values range from $-2{\cdot}8$ to $-21$, indicating that important contributions to the $C$'s are non-coulombic. It is in these differences that the effects of strain on the various contributions to the crystal cohesive energy are sorted out.

Formally, one can write an elastic stiffness at 0°K as the second derivative of the crystal binding energy with respect to the appropriate strain, i.e. $\Omega C = \frac{\partial^2 U_o}{\partial \epsilon^2}$ where $\Omega$ is the crystal volume, $U_o$ the total cohesive energy, $\epsilon$ the strain associated with the constant $C$. The differentiating with respect to ln $r$, $r$ being a distance in the crystal,

$$\frac{\Omega \, \mathrm{d}C}{\mathrm{d} \ln r} + 3\Omega C = \frac{\partial^2 U_o}{\partial \epsilon^2 \partial \ln r}$$

For the sake of definiteness, consider the series: $U_o$, the crystal energy at 0°K, the equilibrium condition, the bulk modulus, and the strain derivative of the bulk modulus, all taken at 0°K, for a simple model of the binding energy of NaCl, following the treatment in Kittel,[29] with modifications and addition of $\mathrm{d}B_T/\mathrm{d} \ln r$. Numbers above the terms in the equations give their relative contributions.

$U_o = N\phi$ where $N$ = number of molecules, $\phi$ = energy per molecule, $U_o$ = crystal energy.

$$U_o = N\left(\overset{1}{\frac{\lambda A_n}{R^n}} - \overset{9}{\frac{\alpha e^2}{R}}\right)$$ a model in which the second term is the electrostatic energy of the assembly of positive and negative ions, the Madelung energy, the first term a repulsive interaction between ion cores, varying as a higher power of $R$, the cation–anion separation in the crystal. $\lambda$, $A_n$, n and $\alpha$ are constants.

Now $p = -\frac{\mathrm{d}U_o}{\mathrm{d}V} = -\frac{\mathrm{d}U_o}{\mathrm{d}R} \cdot \frac{\mathrm{d}R}{\mathrm{d}V}$, $V = 2NR^3$

so that $p = -1/3 \frac{N}{2NR^3}\left[-\frac{n\lambda A_n}{R^n} + \frac{\alpha e^2}{R}\right]$

at the equilibrium spacing, $p = 0$, i.e. $-\overset{1}{\frac{n\lambda A_n}{R^n}} + \overset{1}{\frac{\alpha e^2}{R}} = 0$.

The bulk modulus $B_T = -V\left(\frac{\partial P}{\partial V}\right)_T$

$$B_T = \frac{N}{9V}\left[\overset{3}{(n+3)} \cdot \frac{n\lambda A_n}{R^n} - \overset{1}{\frac{4\alpha e^2}{R}}\right]$$

using n evaluated, 9·4, and equilibrium condition $\frac{n\lambda A_n}{R^n} = \frac{\alpha e^2}{R}$.

**The strain derivative of $B_T$ is given by:**

$$\frac{\mathrm{d}B_T}{\mathrm{d} \ln R} = \frac{N}{9V}\left[-\overset{10}{(n^2+6n+9)} \cdot \frac{n\lambda A_n}{R_n} + \overset{1}{\frac{16\alpha e^2}{R}}\right], \left(= -3\,B_T \frac{\mathrm{d}B_T}{\mathrm{d}P}\right)$$

**Table I**

*Values of the hydrostatic strain derivatives of elastic constants of materials,* $\frac{\mathrm{d}\ln C}{\mathrm{d}\ln r}$.

For reference, values of the elastic constants in units $10^{12}$ dyne cm.$^{-2}$ are placed in parenthesis behind the corresponding strain derivative. The notation $C \equiv C_{44}$, $C' \equiv 1/2(C_{11} - C_{12})$ and $B_s \equiv 1/2\,(C_{11} + 2C_{12})$ has been used.

| | $\frac{\mathrm{d}\ln C}{\mathrm{d}\ln r}$ | | $\frac{\mathrm{d}\ln C'}{\mathrm{d}\ln r}$ | | $\frac{\mathrm{d}\ln B_s}{\mathrm{d}\ln r}$ | |
|---|---|---|---|---|---|---|
| Na | −7·2 | (0·042) | −7·2 | (0·0058) | −10·1 | (0·066) |
| Li | −4·1 | (0·088) | −2·8 | (0·010) | — | (0·012) |
| Al | −17·8 | (0·283) | −15·2 | (0·232) | −14·9 | (0·764) |
| Cu | −12·5 | (0·751) | −9·93 | (0·233) | −16·3 | (1·37) |
| Ag | −15·2 | (0·461) | −12·73 | (0·153) | −18·2 | (1·04) |
| Au | −21·2 | (0·420) | −14·80 | (0·147) | −18·6 | (1·73) |
| Ge | −3·6 | (0·673) | −0·58 | (0·403) | −13·6 | (0·751) |
| Si | −3·0 | (0·796) | −0·30 | (0·511) | −15·3 | (0·993) |
| RbI | +5·8 | (0·0287) | — | (0·112) | — | (0·106) |
| NaCl | −1·84 | (0·128) | −16·7 | (0·184) | −16·4 | (0·245) |
| KCl | +3·35 | (0·630) | −15·9 | (0·170) | −12·2 | (0·184) |

The relative contributions of the short-range repulsion to coulombic terms for each are: short range/long range $U_o$, 1:9; $R_o$, 1:1; $B_T$, 3:1; $\mathrm{d}B_T$, 10:1.

This sequence illustrates the relative increase in the importance of rapidly varying short-range contributions to the binding energy, as successive derivative quantities are considered. This is relevant even in those materials such as the alkali metals where the ion core contribution to the elastic constants is considered unimportant, since the apparent absence of a short-range contribution to the pressure derivatives provides very convincing evidence of its absence as a contributor to the cohesive energy, the equilibrium condition or the elastic constants. The equations for the contribution of the short-range terms (nearest neighbours only) and the coulomb term to the pure shear stiffnesses in the NaCl structure are:

$$C = \frac{N}{V}\left[2R\cdot\frac{\mathrm{d}W}{\mathrm{d}R} + 1{\cdot}28\,\frac{e^2}{R}\right]R = R_o \qquad C' = \frac{N}{V}\left[R^2\cdot\frac{\mathrm{d}^2W}{\mathrm{d}R^2} + R\cdot\frac{\mathrm{d}W}{\mathrm{d}R} - 1{\cdot}33\,\frac{e^2}{R}\right]R = R_o$$

$$\frac{\mathrm{d}C}{\mathrm{d}\ln R} = \frac{N}{V}\left[2R^2\cdot\frac{\mathrm{d}^2W}{\mathrm{d}R^2} + 4\,R\cdot\frac{\mathrm{d}W}{\mathrm{d}R} - 4\times 1{\cdot}28\cdot\frac{e^2}{R}\right]R = R_o$$

$$\frac{\mathrm{d}C'}{\mathrm{d}\ln R} = \frac{N}{V}\left[R^3\cdot\frac{\mathrm{d}^3W}{\mathrm{d}R^3} - 2R\cdot\frac{\mathrm{d}^2W}{\mathrm{d}R^2} + 4\times 1{\cdot}33\cdot\frac{e^2}{R}\right]R = R_o$$

In these equations $W(R)$ is the repulsive interaction energy of the anion–cation pair. The terms containing $e^2/R$ are the electrostatic contributions to the elastic constants and their derivatives and are due to the change of the Madelung energy by shear strain. Note that because of the geometry of the lattice, the term containing $\mathrm{d}^2W/\mathrm{d}R^2$ is absent in the equation for $C$, and the term containing $\mathrm{d}^3W/\mathrm{d}R^3$ is missing from the equation for $\mathrm{d}C/\mathrm{d}\ln r$. For the power-law potential used above, the equations become:

$$C = \frac{N}{V}\left[-2n\cdot\frac{\lambda A_n}{R_o^n} + 1{\cdot}28\cdot\frac{e^2}{R_o}\right], \quad \frac{\mathrm{d}C}{\mathrm{d}\ln r} = \frac{N}{V}\left[(2n^2+6n)\cdot\frac{\lambda A_n}{R_o^n} - 4\times 1{\cdot}28\cdot\frac{e^2}{R_o}\right]$$

$$C' = \frac{N}{V}\left[n^2\cdot\frac{\lambda A_n}{R_o^n} - 1{\cdot}33\cdot\frac{e^2}{R_o}\right], \quad \frac{\mathrm{d}C'}{\mathrm{d}\ln r} = \frac{N}{V}\left[(n^3+3n^2+4n)\cdot\frac{\lambda A_n}{R_o^n} + 4\times 1{\cdot}33\cdot\frac{e^2}{R_o}\right]$$

Physically and macroscopically the elastic constant $C$ can be thought of as the stress–strain ratio for a simple infinitesimal strain changing only the angles between [100] type directions of the crystal and $C'$ as the same ratio for an infinitesimal volume conserving strain generated by compressing one cubic direction of the crystal to $1-\delta$, expanding another to $1/(1-\delta)$. These are shown in Fig. 5. The contributions arise from the second derivative of the crystal energy by

shear strain, and involve considerations of the changes of neighbour distances by the applied strain. The unsophisticated ' power law ' repulsion is considered for illustrative purposes only.

As in the case of the cohesive energy proper, the theory of the elastic constants and their pressure dependence is not completely straightforward.[23] A number of simplifying assumptions must be made for each material considered. We shall however consider some of the structural information which may be derived from the numbers in Table I. The conventional model[34] on which elastic constant calculations are based considers that the only important contributions arise from: (1) a long range coulomb energy (e.g. the Madelung term in ionic crystals), (2) the Fermi energy contributing principally to the bulk modulus in monovalent metals, but important to both shear and bulk moduli in polyvalent metals, and (3) a short-range repulsive interaction between neighbouring closed shell ion cores. The usual treatment considers the short-range repulsion to depend only on $|\bar{r}|$, i.e. the forces are assumed central. The first group of elements listed in Table I is arranged in order of increasing complexity of the interpretation.

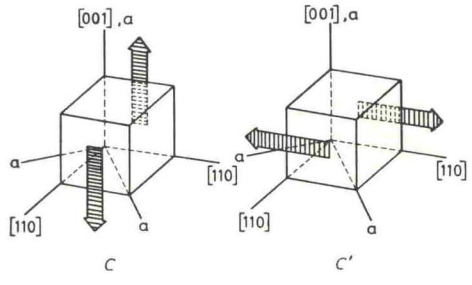


Fig. 5. *Distortions appropriate to* C *and* C′ *shears of a* [110] *crystal*

The $C'$ shear is equivalent to compression along (100) extension (010) while maintaining constant volume

*Sodium*

The shear constants of sodium present the least difficult analysis.[17] The salient features of the sodium data are (1) the elastic anisotropy ratio $C/C'$ does not depend on pressure, (2) the value of the shear strain derivatives is $-7{\cdot}2$. The zero-pressure values of the elastic constants are accounted for quite well by consideration of the electrostatic contribution alone. The theoretical value of the electrostatic contribution calculated by Fuchs[35] on the basis of a model consisting of positive point charges imbedded in a uniform sea of negative charge is:

$$C = \mathrm{K}e^2/r^4, \quad C' = \mathrm{K}'e^2/r^4$$

where K and K′ are geometrical constants, $r$ is the lattice parameter, $e$ the electronic charge. These were modified[36] to take into account variations of charge density in the atomic polyhedron, yielding:

$$C = \mathrm{K}Z^2e^2/r_4, \quad C' = \mathrm{K}'Z^2e^2r^2$$

where $Z$ is the ratio of the charge density at the boundaries of the atomic polyhedron to the value which would obtain if the valence electron charge were uniformly distributed over the cell. The direct ion core interactions in a bcc metal make a *positive* contribution to $C$, a *negative* contribution to $C'$ and would be expected from arguments given before, to contribute relatively more strongly to the strain derivatives. The observation of independence of elastic anistropy on volume indicates with certainty then that the ion core term may be neglected in this analysis. Numerically, one would expect $\dfrac{\mathrm{d}\ln C}{\mathrm{d}\ln r} = -4 = \dfrac{\mathrm{d}\ln C'}{\mathrm{d}\ln r}$ if there were no re-distribution of charge within the atomic polyhedron when the crystal was compressed. The observation that the strain derivative is equal to $-7{\cdot}2$ instead of $-4$ indicates that, as sodium is compressed, the charge density at the cell boundaries increases faster than $1/V$. Analytically this may be expressed as the volume dependence of $Z$, $\dfrac{\mathrm{d}\ln Z}{\mathrm{d}\ln V} = -0{\cdot}54$, or in terms of the volume-dependence of the value of the normalised wave function of the lowest electronic state at the cell boundary, $u_0(\bar{r}_c)$, since $Z = |u_0(\bar{r}_c)|^2$, $\dfrac{\mathrm{d}\ln u_0(\bar{r}_c)}{\mathrm{d}\ln V} = -0{\cdot}27$. Qualitatively this effect may be explained by the consideration that the space within the cell, into which the electron can be compressed as the volume is reduced, is only the space between the ion core and the cell walls (even though the cores in

adjacent cells do not overlap), so the charge density in that space increases more rapidly with compression than would be the case if the electron charge could condense in the entire cell. This effect is predicted theoretically by Brooks,[37,38] but the experimentally observed effect is about twice that of Brooks' theoretical prediction.

*Lithium*

Jain[18] has measured the pressure-dependence of the elastic constants of lithium. Since Cohen & Heine[39] discuss experimental evidence which indicates deviations from sphericity of the Fermi surface in lithium, it was of interest to examine the effects of the Fermi contribution to the pressure dependences of the elastic constants. Jain's measurements yield values $\frac{\mathrm{d}\ln C}{\mathrm{d}\ln r} = -4{\cdot}1$, $\frac{\mathrm{d}\ln C'}{\mathrm{d}\ln r} = -2{\cdot}8$. The observation $\frac{\mathrm{d}\ln C'}{\mathrm{d}\ln r} < \frac{\mathrm{d}\ln C}{\mathrm{d}\ln r}$ suggests at once the presence of a direct ion core interaction, but this can be ruled out by the fact that the ratio of nearest-neighbour separation to ionic diameter is even greater in lithium than in sodium where no ion core effect was found. Jain considers the Fermi contribution to the elastic constants using a modified form of the model applied by Jones[40] to the elastic constants of $\beta$-brass. The analysis indicates (1) the charge-density ratio $Z$ at the atomic cell boundaries increases with decreasing volume as in sodium, but at about half the rate observed in sodium, (2) that the Fermi surface which at zero pressure bulges out about one-third of the distance between the free electron sphere and the [110] planes of the first Brillouin zone[41] becomes more distorted as the pressure is increased. The sign and magnitude of the effect is in good agreement with the work of Blume[42] on the theory of the shear constants in lithium and with Ham's theoretical predictions of the shape of the Fermi surface. The value of the energy gap across the (110) Brillouin zone planes inferred from these data using the model of Cohen & Heine, 0·128 Rydbergs (Ry), compares favourably with theoretical estimates ranging from 0·153 to 0·228 Ry.[41] With Li, important information about the Fermi surface *and its change with volume* is obtained in a simple experiment, information extremely difficult (if not impossible due to the phase transformation in cooling), to obtain directly, e.g. by de Haas–van Alphen measurements carried out at high pressure.

*Aluminium*

As far as one is concerned with a study of the Fermi contribution to elastic constants, aluminium is the classical example, for which the theory has been worked out by Leigh.[43] Schmunk & Smith[15] reworked the theory with better values of the elastic constants of aluminium, and in addition considered the effects of pressure. Two of the three valence electrons in aluminium can occupy the region contained by the first Brillouin zone (shown in Fig. 6), but the third must overlap into the second zone at points indicated by S and H on the Figure. The shear elastic constants are made up of (1) an electrostatic contribution of the form $C = \mathrm{K}\,Z^2e^2/r^4, C' = K'Z^2e^2/r^4$ as for sodium and lithium, and (2) the contribution due to change of the Fermi energy by a shear strain. The ion core interaction is supposed to be an unimportant contributor because of the large ratio of nearest-neighbour distance to ionic diameter. The Fermi contribution is broken down into a contribution from the full zone, evaluated with use of a free-electron expression for the energy, plus a contribution due to the electrons in overlap positions S and H. In considering the contribution of the latter, one must take into account relaxation effects caused by redistribution of the electrons during shear by a transfer from higher to lower energy positions, an effect illustrated in Fig. 7b and 7c which shows a cross-section of the Brillouin zone and the shifts of electron populations with applied $C$ and $C'$ strains. Table III shows values of these contributions to the elastic constants.

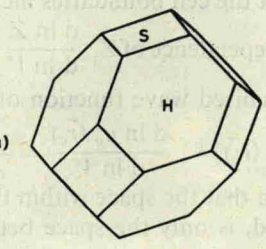


**Fig. 6.** *The Brillouin zone of aluminium, showing positions of electron overlap*

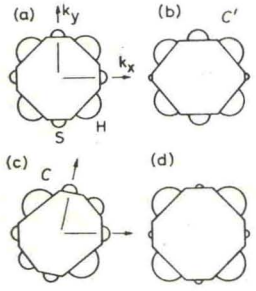


Fig. 7. *Schematic representation of the Brillouin zone and overlap electron populations of aluminium in various strains states*

Electron-overlap populations for the square and hexagonal faces are denoted by S and H respectively.

(a) Unstrained, (b) $C'$ shear strain, (c) $C$ shear strain, and (d) negative volume strain.

as shown in Fig. 7d. Numerically the values correspond to approximate fractional changes 0·002 and − 0·03 respectively in $n_H$ and $n_S$ for a pressure of 10 kb. ($n_H$ and $n_S$ are the number of electrons per atom overlapping each pair of hexagonal or square faces of the Brillouin zone). It is difficult quantitatively to assess the changes of interpretation brought about by use of a ' more modern ' Fermi surface, that described by Harrison.[44] Qualitatively however, the Harrison Fermi surface which implies nearly free electrons leaves the difficulty of accounting for the *observed elastic isotropy* $C \simeq C'$ in aluminium. A completely ' free electron ' model, i.e. a model giving a spherical Fermi surface, leads to zero Fermi contributions to the pure shear stiffnesses. If the Fermi contribution to $C$ and $C'$ is negligible, then the anisotropy ratio $C/C'$ would have approximately the value obtained by consideration of the electrostatic contributions only, i.e. about 9 instead of the experimentally observed value 1·22.

**Table III**

*Constitution of the present observed shear stiffnesses of aluminium as explained by Leigh's model*

(units are $10^{12}$ dyne cm.$^{-2}$)

| Contribution | $C$ | | $C'$ | |
|---|---|---|---|---|
| Coulomb ($C_E$) | | 1·106 | | 0·1235 |
| Fermi: Full zone | 0·450 | | 0·1500 | |
| Hexagonal overlap | −1·320 | | 0·5400 | |
| Square-face overlap | 0·047 | | −0·5817 | |
| Net Fermi ($C_F$) | | −0·823 | | 0·1083 |
| Total (observed) ($C_E + C_F$) | | 0·283 | | 0·232 |

The notable feature of Leigh's theory is that it *accounts for the near equality of* C *and* C′ which is remarkable when one considers that the electrostatic contribution taken alone has an anisotropy ratio $C/C'$ of about 9. Table IV contains the contributions of these terms to the strain derivatives of $C$ and $C'$. Qualitatively this interpretation indicates (1) as in the cases of sodium and lithium, the charge density at the boundaries of the atomic polyhedra increases as aluminium is compressed. In terms of the volume dependence of $Z$, $\frac{\mathrm{d} \ln Z}{\mathrm{d} \ln V} = -0{\cdot}78$, a larger value than found in sodium; (2) as the pressure is applied to the specimen, part of the electrons in states overlapping the square faces of the Brillouin zone transfer to states overlapping the hexagonal faces

**Table IV**

*Values for aluminium of the contributions* $(-\mathrm{d}C_i/\mathrm{d} \ln r)/C$ *to the derivatives* $(-\mathrm{d} \ln C/\mathrm{d} \ln r)$ *of the shear stiffnesses* C *and* C′

The quantities $(-\mathrm{d}C_i/\mathrm{d} \ln r)/C$ arise from the contributions, $C_i$ which are named.

| Contribution | $C$ | $C'$ |
|---|---|---|
| Coulomb term | 34·13 | 4·65 |
| Net Fermi term assuming n constant | −14·52 | 2·32 |
| Contributions from electron transfer with volume strain | | |
| Hexagonal overlap | − 0·17 | 1·59 |
| Square-face overlap | − 1·62 | 6·63 |
| Total (and observed) | 17·8 | 15·2 |

*Copper, silver and gold*

The monovalent noble metals copper, silver and gold represent a class of metals in which the elastic properties are dominated by the overlapping of nearest-neighbour ion cores. It is well known that these repulsive short-range interactions must be introduced to account for the low value of the observed compressibility. Almost all of our experimental knowledge of the ostensible form of the ion core interactions is derived from the elastic constants. The short-range interaction is an important one in the theory of diffusion in copper and several workers in this field have followed[45–47] the procedure of evaluating the repulsion parameters from the observed values of the elastic constants. This is reasonably satisfactory for the purpose, but attempting to account for the elastic constants of copper in detail in terms of a two-parameter exponential repulsion is less satisfactory. This failure is seldom pointed out explicitly, but it becomes more and more apparent when one examines the single-crystal elastic stiffness of the similar metals silver and gold. As pointed out earlier, the importance of a short-range interaction becomes more accentuated as one examines its contribution to each of the sequence: binding energy, the equilibrium condition, the elastic stiffnesses and finally the pressure derivatives of the elastic stiffnesses which will be determined almost entirely by the ion core repulsions in these metals. The original goals of the copper, silver, gold investigation which was our first high-pressure venture, were twofold. First we wished to obtain volume dependencies of the elastic constants for use in 'correcting' to constant volume experimental data on effects of dilute alloying on elastic constants, i.e. to separate out the specific effects of alloying, from the effects due to change of lattice parameter on alloying. An example of the use of this correction is found in an article by Schmunk & Smith on elastic constants of copper–nickel alloys.[48] The second goal was to study the ion core interactions in detail under the favourable conditions that they made the largest contributions to the quantities measured. It was assumed that the stiffnesses were made up by (1) the electrostatic contribution and (2) the ion core interaction. At that time there was much less evidence than at present indicating the distortion of the Fermi surfaces from spherical. Accordingly it was assumed that $E_F$ made no contribution to the shear constants or their strain derivatives, but that it did contribute to the bulk modulus. Inclusion of a Fermi term would not be very likely to affect the qualitative conclusions reached in our interpretation. Briefly, the study of the ion core interactions at close range, i.e. via the pressure derivatives of the elastic constants reveals serious failure of the assumption made in conventional elastic constant theory that the ion core interactions are central, i.e. that they act along the line between ion core centres. The failure becomes much more apparent as one considers in turn the behaviour of copper, silver and gold. The failure of the assumption of centrality of the interactions is so severe, that no reasonable extension may usefully be made of the usual consideration that the bulk modulus of the electron gas is responsible for failure of the Cauchy relations to hold in these metals.

*Germanium and silicon*

No thorough treatment of the elastic constants of the diamond-like semiconductors in terms of their cohesive energy has been advanced. Implications regarding their thermal properties are discussed later.

*Rubidium iodide*

This salt is in this list although measurements on it are not complete at this time. Buerger proposes a mechanism of finite $C_{44}$ type strain to describe the CsCl–NaCl structure transitions.[49,19] We thought it possible that the transformation in rubidium iodide (RbI) took place by loss of stability with respect to a $C_{44}$ shear, i.e. that $C_{44}$ would vanish at the transformation pressure as apparently happens in AuCd. Merely a 10% decrease in $C_{44}$ is observed in compressing to the transformation pressure, ruling out that possibility. It is hypothesised that the structure becomes unstable by the vanishing of one of the *short wave-length* lattice frequencies in a mode of the $C_{44}$ type (transverse acoustic [100] in more usual nomenclature). The thermal diffuse scattering of *X*-rays by RbI as a function of pressure is now being examined and, if the hypothesis holds, a large *change* is expected in thermal diffuse scattering from the modes whose frequency vanishes at the transformation pressure. Also, there should be a negative anomaly in the thermal expansion coefficient of RbI at low temperatures, due to negative dependence on applied pressure of those mode frequencies, as will be more generally discussed later.

**(3) Thermal aspects**

In addition to the use of the pressure-dependence of the elastic constants to augment other investigations of cohesion in solids, the data are directly applicable to the study of certain aspects of anharmonicity of lattice vibrations. Consider the acoustic wave velocity and its pressure dependence in terms of the dispersion curves for lattice vibrations of a solid as revealed in the plot of the frequency vs. $|\bar{\mathbf{k}}|$ where $\bar{\mathbf{k}}$ is the wave vector for some direction of propagation in the crystal (see Fig. 8). The initial slope of such a curve is the velocity of an acoustic wave of frequency low compared to the cut-off frequency $\nu_{max}$. Typical cut-off frequencies are $\sim 10^{13}$ cycles per second so that our 10-mc search wave is very near the origin on the scale of Fig. 8 and information derivable from it will only be applicable over the region of the $\nu$ vs. $|\bar{\mathbf{k}}|$ curve non-dispersive at all pressures considered. Consider now the behaviour of a normal mode $i$ lying in the non-dispersive region (see Fig. 8), i.e. a plane standing-wave having a fixed number of nodes between two atom sites a distance $L$ apart and a frequency $\nu_i$. As the crystal volume is changed by application of pressure, the mode frequency will change for two reasons: (1) the sound velocity, hence the slope of the curve, will change, and (2) the value of $|\bar{\mathbf{k}}|$ will change because the reference lattice sites are compressed with the crystal. Analytically one can express this dependence in terms of $\gamma_i \equiv -\dfrac{\mathrm{d}\ln\nu_i}{\mathrm{d}\ln V}$, from which a connection may be made to the pressure dependence of the elastic constants by the relations: $v_i = \nu_i k_i$ where $v_i$ is the wave velocity appropriate

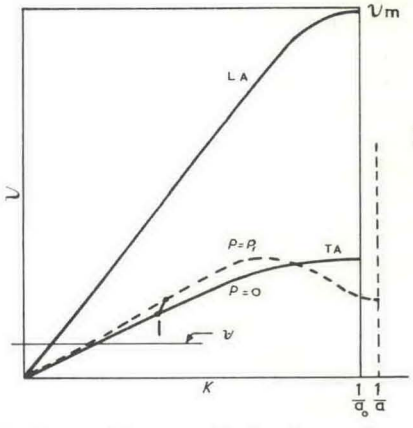


Fig. 8. *Acoustic lattice vibration dispersion curves for a longitudinal mode (LA) and a transverse mode (TA), showing change of the transverse acoustic (TA) curve caused by an applied pressure* $P_1$, *and the shift in frequency of the i'th normal mode*

The horizontal line, cutting off the frequency at $\nu = kT/h$ indicates the fact that at low temperatures, only the modes with less than this frequency are active

to type of wave, $k_i$ is the reciprocal of the wavelength of the mode under consideration, $v_i = (C_i/\rho)^{\frac{1}{2}}$ where $C_i$ is an elastic stiffness appropriate to the wave type, $\rho$ the crystal density, and finally $\dfrac{\mathrm{d}\ln C_i}{\mathrm{d}\ln V} = -\dfrac{B\,.\,\mathrm{d}C_i}{C_i\,.\,\mathrm{d}P}$. Geometrically $\dfrac{\mathrm{d}\ln k_i}{\mathrm{d}\ln V} = -\dfrac{1}{3}$, $\dfrac{\mathrm{d}\ln\rho}{\mathrm{d}\ln V} = -1$. Performing the necessary derivatives and combining terms yields $\gamma_i = -\dfrac{1}{2}\cdot\dfrac{\mathrm{d}\ln C_i}{\mathrm{d}\ln V} - \dfrac{1}{6}$, an equation resembling the familiar expression* due to Slater,[5] but with $C_i$ replaced by $B_T$, the bulk modulus, and derived under somewhat different restrictions: $\gamma_s = -\dfrac{1}{2}\cdot\dfrac{\mathrm{d}\ln B_T}{\mathrm{d}\ln V} - \dfrac{1}{6}$. Note that applicability of the Slater $\gamma$ depends sensitively on independence of Poisson ratios on volume. If one has only a set of lattice vibrational modes $\gamma_i$ contributing appreciably to the heat capacity of the crystal at the temperature under consideration, i.e. the electronic or other contributions may be neglected, a good approximation in insulators and semiconductors, one can, following Slater,[5] or Peierls[50] assume that the free energy of the crystal can be written:

$F = U_o(V) + kT\ln Z_{vib.}$ where $U_o(V)$ is the internal energy of the crystal at absolute zero,

* Slater's expression $\gamma_s = a_2/a_1^2 - 2/3$ may be shown to be identical to this expression. Consider $a_1$ and $a_2$ defined by $\Delta V/V_o = a_1P + a_2P^2$, a form in which many of Bridgman's experimental results are stated. Then by solving for $P$ and evaluating $B_T = -V\left(\dfrac{\partial V}{\partial V}\right)_T$ and $\dfrac{\mathrm{d}\ln B_T}{\mathrm{d}\ln V}$ with care to differentiate $B_T(V) = -V\left(\dfrac{\partial P}{\partial V}\right)_T$, not $B_T(V) = V_o\left(\dfrac{\partial P}{\partial V}\right)_T$, $\left(\dfrac{a_2}{a_1^2} - \dfrac{2}{3}\right)$ and $\left(-1/2\dfrac{\mathrm{d}\ln B_T}{\mathrm{d}\ln V} - 1/6\right)$ are seen to be equivalent.

and is assumed to include the zero point energy. $U_o$ is assumed to have no explicit temperature dependence. $Z_{vib.}$ is the quantum mechanical sum over states of the lattice vibrational energies. By elementary statistical mechanics, it can be shown that Grüneisen's gamma, defined by $\gamma_{Gr} = \alpha B_T V/C_v$ (where $\alpha$ is the volume coefficient of thermal expansion, $B_T$ the bulk modulus and $V$ and $C_v$ the volume and heat capacity per mole), is given in terms of the $\gamma_i$ by $\gamma_{Gr} = \dfrac{\Sigma\, C_{vi}\,\gamma_i}{\Sigma\, C_{vi}}$, where $C_{vi}$ is the Einstein heat capacity of the i'th normal mode at the temperature under consideration and the summation is made over all modes. At temperatures $T \gg h\,\nu_{max}$ /k, all modes will have heat capacity k and $\gamma_{Gr} = \bar{\gamma}$, the average of $\gamma_i$ over all modes. In the limit of very low temperatures on the other hand, only the low-frequency acoustic modes will contribute to the heat capacity, the least stiff mode types being the most important contributors. In terms of the dispersion curves shown in Fig. 8, it is seen that if the occupation is cut off at $\nu = kT/h$, then for the lower stiffness modes (lower slope of $\nu$ vs. k), a larger number of states will be contributing to the heat capacity, hence the $\gamma_i$ of these states will contribute relatively more heavily to $\gamma_{Gr}$. Experimentally (see Table V), it is most commonly observed that the lower stiffness modes have smaller $\gamma_i$, hence $\gamma_{Gr}$ should decrease at low temperatures. This has been considered by Sheard[51] for a number of materials, and since one can show[29] that if the low-temperature limit of $\gamma$ be $\gamma_o$, then $\gamma_o = -\dfrac{\mathrm{d}\ln\Theta_o}{\mathrm{d}\ln V}$. Then it is possible very simply to use deLaunay's tables[52] for $\Theta$ ($C_{11}$, $C_{12}$, $C_{44}$, $\rho$) together with values of the $C$'s and d $C$/d$P$'s in order to evaluate the $\gamma_o$, sometimes with surprising results,[53] as in the case of germanium and silicon[54] indicated in Fig. 9. Of course, one expects this value to be a valid one only in the case of materials in which one can assume negligible contribution of electronic heat capacity, i.e. in the case of non-metals. The generalisations of this are discussed by Bernardes & Swenson.[55] It is useful also to examine and compare values of $\gamma$ derived with the assumption that the volume-dependence of the frequencies of a particular mode type, e.g. transverse acoustic, is the same in the dispersive region as that for the low-frequency modes. This involves averaging of three $\gamma_i$ (one longitudinal, two transverse) over all directions in the crystal. Some values of $\bar{\gamma}$ are shown in Table V comparing $\gamma_{Gr}$, $\gamma_s$, and $\bar{\gamma}$ derived from shear and longitudinal acoustic measurements. Agreement of $\bar{\gamma}$ with $\gamma_{Gr}$ is excellent in most cases, indicating that probably the gammas for modes in the dispersive region do not differ widely from those measured in the low frequency part of the lattice vibrational spectrum. A spectacular exception to the latter is provided by the temperature dependence of $\gamma_{Gr}$ in the case of the diamond-like structures, e.g. Ge, Si, InSb, as shown in Fig. 9. In these a very pronounced dip in $\gamma_{Gr}$ appears at about a tenth of the Debye temperature. The interpretation[56] of these negative anomalies is that the dispersive part of the spectrum of the transverse acoustic modes

**Table V**

$\gamma_i = -\dfrac{\mathrm{d}\ln\nu_i}{\mathrm{d}\ln V}$ *for various long wavelength acoustic mode types*

Values of the elastic constants appropriate to these modes are given in units $10^{12}$ dyne cm$^{-2}$. Comparison is made between the average $\gamma_1$ for these simple modes, the Slater $\gamma$ and the Grüneisen $\gamma$, $\gamma_{Gr} = \alpha B_T V/C_v$, showing the better agreement between $\gamma_{Gr}$ and $\gamma_s$. $\bar{\gamma}$ for NaCl and KCl are taken from Sheard[51] and represent an average of $\gamma_i$ over all directions of propagation. $\Theta$ is the Debye temperature.

| Crystal | $C'_{11}$ | $C_{44}$ | $C'$ | $\gamma'_{11}$ | $\gamma_{44}$ | $\gamma'$ | $\bar{\gamma}$ | $\alpha B_T V/C_v$ $= \gamma_{Gr}$ | Slater $\gamma$ | $\gamma_o$ | $T/\Theta$ |
|---|---|---|---|---|---|---|---|---|---|---|---|
| Na | 0·11 | 0·42 | 0·0058 | 1·36 | 1·06 | 1·06 | 1·16 | 1·16 | 1·5 | | 1·9 |
| Cu | 2·25 | 0·75 | 0·23 | 2·30 | 1·92 | 1·49 | 1·90<br>1·97 | 1·96 | 2·55 | 1·80 | 0·9 |
| Ag | 1·60 | 0·46 | 0·15 | 2·69 | 2·38 | 1·96 | 2·34 | 2·40 | 2·85 | | 1·3 |
| Au | 2·30 | 0·42 | 0·15 | 3·00 | 3·38 | 2·31 | 2·90 | 2·90 | 2·93 | | 1·8 |
| Al | 1·19 | 0·28 | 0·23 | 2·43 | 2·80 | 2·36 | 2·53<br>2·57H | 2·27 | 2·31 | 2·90 | 0·8 |
| Ge | 1·56 | 0·67 | 0·40 | 1·27 | 0·58 | 0·17 | 0·72 | ~0·73 | 2·1 | 0·49 | ~0·5 |
| Si | 2·11 | 0·79 | 0·50 | 1·35 | 0·33 | −0·13 | 0·51 | ~0·45 | 2·5 | 0·25 | ~0·45 |
| $SiO_2$ fused | | | | −2·40 | ~−2·08 | ~−2·08 | −2·19 | ~0·00 | | | |
| NaCl | 0·486 | 0·128 | 0·184 | 1·99 | 0·14 | 2·89 | 1·60S | 1·60 | 1·52 | 1·23 | |
| KCl | 0·307 | 0·063 | 0·165 | 1·81 | −0·87 | 3·03 | 1·57S | 1·48 | 1·26 | 0·53 | |
| RbI | 0·171 | 0·028 | 0·112 | — | −1·15 | — | | | | | |

S taken from Sheard[51] and H average by Houston's method

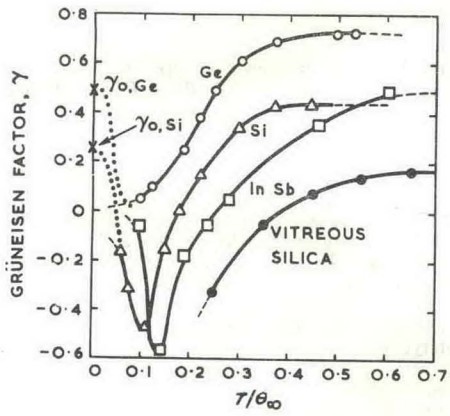


Fig. 9. *Variation of Grüneisen factor with reduced temperature* $T/\theta_\infty$ *for germanium* ($\theta_\infty = 400°K$), *silicon* ($\theta_\infty = 495°K$) *and indium antimonide* ($\theta_\infty = 214°K$)

in these materials exhibits behaviour qualitatively like that shown on Fig. 8 for the transverse acoustic mode, i.e. those mode frequencies in the dispersive region which exhibit an anomalous volume-dependence, their frequencies decreasing as the crystal is compressed. This behaviour of $\gamma_{Gr}$, quite general in the materials with zinc blende structure,[57] stresses a fundamental limitation of the acoustic method for examining simple anharmonicity revealed by the low-frequency acoustic $\gamma$'s, namely that experimental restrictions placed by the frequency limit of the measurements, $\sim$ 10 mc, confine the obtainable information to the non-dispersive region. An ideally direct means of circumventing the restriction will be to perform slow-neutron diffraction[58] experiments on crystals in the high-pressure ambient. As yet this is a virgin field for endeavour which may not present impossible difficulties when tried. It is also possible that thermal diffuse scattering of *X*-rays by materials at high pressures may provide information about *changes* of the shape of the vibrational spectrum in those materials where large charges are to be expected. We are trying to estimate changes in thermal diffuse scattering in RbI crystals as the NaCl $\rightarrow$ CsCl structure transformation pressure is approached, in order to verify our hypothesis of large negative $\gamma$'s for certain TA modes (see section headed Rubidium Iodide). A further *simple* experiment to investigate the volume dependence of the modes, with propagation vector extending to the [100] zone boundary in germanium is also being tested. This experiment seeks to measure directly the pressure shift of the phonon kinks in tunnel diode characteristics at very low temperatures,[59] thus using a simple electrical measurement to give values of $\gamma$ for these modes, especially to verify the qualitative analysis that the $\gamma$'s of those transverse acoustic modes will be negative.

**Acknowledgment**

The authors would like to thank Professors R. Smoluchowski and B. S. H. Royce for helpful advice in constructing this paper.

**References**

[1] Wigner, E., & Seitz, F., *Phys. Rev.*, 1934, **46**, 509
[2] Frohlich, H., *Proc roy. Soc.*, [A], 1937, **158**, 97
[3] Bardeen, J., *J. chem. Phys.*, 1938, **6**, 367
[4] Bardeen, J., *J. chem. Phys.*, 1938, **6**, 372
[5] Slater, J. C., 'Introduction to Chemical Physics', 1939, Chapter XII, Section 4 (New York: McGraw-Hill)
[6] Swenson, C. A., 'Solid State Physics', 1960, **11**, pp. 41—147 (New York: Academic Press Inc.)
[7] Birch, F., *J. appl. Phys.*, 1937, **8**, 129
[8] Hughes, D. S., & Cross, J. H., *Geophysics*, 1951, **16**, 577
[9] Hughes, D. S., & Maurette, C., *J. appl. Phys.*, 1956, **27**, 1184
[10] Lazarus, D., *Phys. Rev.*, 1949, **76**, 545
[11] McSkimmin, H. J., *J. acoust. Soc. Amer.*, 1957, **30**, 314
[12] Anderson, O. L., in 'Progress in Very High Pressure Research', eds. Bundy, F. P., *et al.*, 1961, pp. 225—255 (New York: John Wiley and Sons, Inc.)
[13] Voronov, F. F., Vereschagin, L. F., & Koncharova, V. A., *Dokl. Akad. Nauk SSSR*, 1960, **135**, 1104
[14] Daniels, W. B. & Smith, Charles S., *Phys. Rev.*, 1958, **111**, 713
[15] Schmunk, R. E., & Smith, Charles S., *J. Phys. Chem. Solids*, 1959, **9**, 100
[16] Chapman, J., Masters Thesis, Case Institute of Technology, Cleveland, Ohio, 1959
[17] Daniels, W. B., *Phys. Rev.*, 1960, **119**, 1246
[18] Jain, A. L., *Phys. Rev.*, 1961, **123**, 1234
[19] Daniels, W. B., *Bull. Amer. phys. Soc.*, 1962, **7**, (March)
[20] Huntington, H. B., *Phys. Rev.*, 1947, **72**, 321
[21] Neighbours, Bratten & Smith, *J. appl. Phys.*, 1952, **23**, 389
[22] McSkimmin, H. J., *J. appl. Phys.*, 1953, **24**, 988
[23] Huntington, H. B., 'Solid State Physics', 1960, **7**, pp. 213—351, (New York: Academic Press Inc.)
[24] Jacobs, I. S., *Phys. Rev.*, 1953, **93**, 993
[25] Daniels, W. B., & Hruschka, A. A., *Rev. sci. Instrum.*, 1957, **28**, 1058

**References** (*continued*)


[26] Bridgman, P. W.,' Physics of High Pressure ', 1952, Chap. 6 (London: G. Bell & Sons)
[27] Bridgman, P. W., *Proc. Amer. Acad.*, 1940, **74**, 11
[28] Eros, S. & Reitz, J. R., *J. appl. Phys.*, 1958, **29**, 683
[29] Kittel, C., ' Introduction to Solid State Physics ' 1956, (New York: John Wiley & Sons)
[30] Corll, J. A., *Office of Naval Res. Tech. Rep.*, 1961, (Feb.), No. 5, Contract Nonr–1141 (05), Project NR 017—309
[31] Hinrichs, C. H., & Swenson, C. A., *Phys. Rev.*, 1961, **123**, 1106
[32] Dugdale, J. S., & Hulbert, J. A., *Canad. J. Phys.*, 1957, **35**, 720
[33] Bernstein, B., private communication
[34] Mott, N. F., in ' Progress in Metal Physics ', ed. Bruce Chalmers, 1952, **3**, pp. 90—94 (New York: Interscience Publishers Inc.)
[35] Fuchs, K., *Proc. roy. Soc.*, [A], 1936, **153**, 622
[36] Fuchs, K., *Proc. roy. Soc.*, [A], 1936, **157**, 444
[37] Brooks, H., *Phys. Rev.*, 1958, **112**, 344
[38] Brooks, H., *Phys. Rev.*, 1953, **91**, 1028
[39] Cohen, M. H., & Heine, V., *Adv. Phys.*, 1958, **7**, 395
[40] Jones, H., *Phil. Mag.*, 1952, **43**, 105
[41] Ham, F. S., ' The Fermi Surface ', ed. Harrison & Webb, 1960, pp. 9—27 (New York: John Wiley & Sons Inc.)
[42] Blume, M., Ph.D. Thesis, Harvard University, 1959
[43] Leigh, R. S., *Phil. Mag.*, 1951, **42**, 139
[44] Harrison, W. A., as reference 41, pp. 28—38
[45] Huntington, H. B., & Seitz, F., *Phys. Rev.*, 1942, **61**, 315
[46] Huntington, H. B., *Phys. Rev.*, 1953, **91**, 1092
[47] Zener, C., *Acta cryst.*, 1950, **3**, 346
[48] Schmunk, R. E., & Smith, Charles S., *Acta metallurg.*, 1960, **8**, 396
[49] Buerger, R. M., in ' Phase Transformations in Solids ', eds. Smoluchowski, Mayer & Weyl, 1958, pp. 183—209 (New York: John Wiley & Sons Inc.)
[50] Peierls, R., ' Quantum Theory of Solids ', 1955 (Oxford University Press)
[51] Sheard, F. W., *Phil. Mag.*, 1958, **3**, 138
[52] deLaunay, J., ' Solid State Physics '. 1960, **2**, pp. 219—303 (New York: Academic Press Inc.)
[53] Daniels, W. B., *Phys. Rev. Letters*, 1962, **8**, 3
[54] Gibbons, D. F., *Phys. Rev.*, 1958, **112**, 136
[55] Bernardes, N., & Swenson, C. A., ' The Equation of State of Solids at Low Temperatures ', to be published.
[56] Daniels, W. B., *Proc. Conf. on Semiconductor Physics*, 1962, to be published
[57] Novikova, S. I., *Soviet Physics Solid State*, 1960, **2**, 37, 1464, 2087; 1961, **3**, 129
[58] Brockhouse, B. N., & Iyengar, P. K., *Phys. Rev.*, 1958, **111**, 747
[59] Holonyak, Lesk, Hall, Tiemann & Ehrenreich, *Phys. Rev. Letters*, 1959, **3**, 167